

Cite this: *RSC Adv.*, 2018, 8, 10148

# GSH-doped GQDs using citric acid rich-lime oil extract for highly selective and sensitive determination and discrimination of $\text{Fe}^{3+}$ and $\text{Fe}^{2+}$ in the presence of $\text{H}_2\text{O}_2$ by a fluorescence “turn-off” sensor

Khanitta Saenwong,<sup>a</sup> Prawit Nuengmatcha,<sup>b</sup> Phitchan Sricharoen,<sup>a</sup>  
Nunticha Limchoowong<sup>a</sup> and Saksit Chanthai<sup>id</sup>\*<sup>a</sup>

Synthesis and characterization of graphene quantum dots (GQDs) simultaneously doped with 1% glutathione (GSH-GQDs) by pyrolysis using citric acid rich-lime oil extract as a starting material. The excitation wavelength ( $\lambda_{\text{max}} = 337 \text{ nm}$ ) of the obtained GSH-GQD solution is blue shifted from that of bare GQDs ( $\lambda_{\text{max}} = 345 \text{ nm}$ ), with the same emission wavelength ( $\lambda_{\text{max}} = 430 \text{ nm}$ ) indicating differences in the desired N and S matrices decorating the carbon based nanoparticles, without any background effect of both ionic strength and masking agent. For highly  $\text{Fe}^{3+}$ -sensitive detection under optimum conditions, acetate buffer at pH 4.0 in the presence of  $50 \mu\text{M}$   $\text{H}_2\text{O}_2$ , the linearity range was  $1.0\text{--}150 \mu\text{M}$  ( $R^2 = 0.9984$ ), giving its calibration curve:  $y = 34.934x + 169.61$ . The LOD and LOQ were found to be  $0.10$  and  $0.34 \mu\text{M}$ , respectively. The method's precisions expressed in terms of RSDs for repeatability ( $n = 3 \times 3$  for intra-day analysis) were  $2.03$  and  $3.17\%$  and for reproducibility ( $n = 5 \times 3$  for inter-day analysis) were  $3.11$  and  $4.55\%$  for  $\text{Fe}^{2+}$  and  $\text{Fe}^{3+}$ , respectively. The recoveries of the method expressed as the mean percentage ( $n = 3$ ) were found in the ranges of  $100.1\text{--}104.1$  and  $98.08\text{--}102.7\%$  for  $\text{Fe}^{2+}$  and  $\text{Fe}^{3+}$ , respectively. The proposed method was then implemented satisfactorily for trace determination of iron speciation in drinking water.

Received 18th December 2017  
Accepted 17th February 2018

DOI: 10.1039/c7ra13432k

rsc.li/rsc-advances

## 1. Introduction

Iron (Fe) is a metal of biological, clinical, environmental, and industrial importance. It is one of the most essential trace elements in living biosystems and plays indispensable and versatile roles in many physiological and pathological processes, including enzyme catalysis, oxygen transport, cellular metabolism, electron transfer, and DNA and RNA synthesis.<sup>1–5</sup> Speciation of iron, an occurrence of the element in two oxidation states (II and III), is mostly found in nature. Different biological activities of  $\text{Fe}^{2+}$  and  $\text{Fe}^{3+}$  are well known.  $\text{Fe}^{2+}$  is favored for absorption by biological cells. To treat clinical symptoms of iron deficiency some medicaments containing  $\text{Fe}^{2+}$  can be administrated to eliminate complications. The low stability of  $\text{Fe}^{2+}$  caused by its easy oxidation to  $\text{Fe}^{3+}$  by oxygen in the air can result in a decrease in the real  $\text{Fe}^{2+}$  concentration in

pharmaceuticals.<sup>6</sup> However, both a deficiency and an excess accumulation of iron in the human body can induce serious disorders such as anaemia, intelligence decline, arthritis, heart failure, diabetes and cancer.<sup>7–9</sup> Thus, the determination of iron speciation is of fundamental importance for the early identification and diagnosis of these diseases. In addition, the measurement of iron concentration in water samples is also crucial for environmental safety.<sup>10</sup>

Currently, several analytical techniques for determination of  $\text{Fe}^{2+}$  and  $\text{Fe}^{3+}$  ions have been applied including solid phase extraction,<sup>11</sup> fiber-optic chemosensor,<sup>12</sup> voltammetric methods,<sup>13</sup> high performance liquid chromatography,<sup>14</sup> capillary electrophoresis,<sup>15</sup> inductively coupled plasma mass spectrometry,<sup>16</sup> flow injection analysis<sup>17</sup> and chemiluminescence.<sup>18</sup> Although these techniques are highly sensitive and selective, they require tedious sample preparation and preconcentration procedures, expensive instruments, and professional personnel.

In recent years, several fluorescence sensors have been widely investigated for the selective detection of iron speciation in biological systems because of their ability to provide a simple, sensitive, and selective method for monitoring without the need for any pretreatment of the sample; these techniques also have the advantages of spatial and temporal

<sup>a</sup>Materials Chemistry Research Center, Department of Chemistry, Center of Excellence for Innovation in Chemistry, Faculty of Science, Khon Kaen University, Khon Kaen 40002, Thailand. E-mail: sakcha2@kku.ac.th

<sup>b</sup>Nanomaterials Chemistry Research Unit, Department of Chemistry, Faculty of Science and Technology, Nakhon Si Thammarat Rajabhat University, Nakhon Si Thammarat 80280, Thailand



resolution.<sup>19–21</sup> Therefore, the development of a novel fluorescence probe with low cytotoxicity, excellent biocompatibility, and high water solubility has become increasingly important and urgent. Recently, graphene quantum dots (GQDs) have ignited increasing research interest as an exciting class of carbon nanomaterial, and have emerged as a potential new platform in designing and tuning fluorescence (FL) biosensing and imaging.<sup>22–35</sup> GQDs were discovered very recently as a class of zero-dimensional graphitic nanomaterials with lateral dimensions less than 100 nm in single layers, double layers and few layers (3 to <10).<sup>36–39</sup> Moreover, similar to graphene nanosheets, GQDs have excellent characteristics such as large surface area, large diameter, fine surface grafting *via* the  $\pi$ – $\pi$  conjugated network or surface groups and other special physical properties.<sup>40,41</sup> Furthermore, the carboxyl and hydroxyl groups at their edge enable them to display the excellent properties of high biocompatibility, low toxicity, chemical inertness and good water-solubility for successive functionalization with various organic, inorganic, polymeric or biological species.<sup>42–46</sup> On the basis of these unique properties, various GQD-based fluorescence probes for the detection of metal ions ( $\text{Fe}^{3+}$ ,  $\text{Cu}^{2+}$ , or  $\text{Pb}^{2+}$ ),<sup>35–37</sup> small organic molecules (2,4,6-trinitrotoluene or *para*-nitrophenol)<sup>47,48</sup> and biomaterials (pyrocatechol, human immunoglobulin G, or protein kinase)<sup>49–51</sup> have been explored. The major disadvantage of GQD-based fluorescence probes is that the sensitivity and selectivity are limited due to the non-specificity of GQDs.<sup>52–54</sup> Doping GQDs with heteroatoms can effectively modulate their band gap and electronic density, enhancing the chemical activity of GQDs for practical applications, which has been proven through theoretical calculations and detailed experiments.<sup>55–59</sup> For example, nitrogen-doped GQDs (N-GQDs) showed efficient electrocatalytic activity for the oxygen reduction reaction<sup>46</sup> and cellular and deep-tissue imaging.<sup>60,61</sup> Boron-doped GQDs (B-GQDs) gave rise to rich fluorescence owing to their peculiar interaction with the surrounding media.<sup>62</sup> Sulfur-doped graphene quantum dots (S-GQDs) showed a stable blue-green fluorescence, drastically improved electronic properties, and increased surface chemical reactivity compared with undoped GQDs.<sup>63</sup>

Towards this target, a lot of synthesis methods for various functionalized and non-functionalized GQDs have been established in recent years. Some toxic small organic molecules have been employed to fabricate GQDs using multistep oxidative condensation reactions in organic solutions. In most cases, however, these organic synthetic methods suffer from some disadvantages, such as harsh reaction conditions, high prices, tedious processes, and the use of toxic starting materials.<sup>64–68</sup> In this regard, searching for precursors from regular food may provide green routes that could overcome the above mentioned drawbacks. Some natural foods have been consumed by human beings for centuries, and are still very common in daily life. If natural food could be used as a non-toxic starting material for the synthesis of GQDs, such eco-friendly synthesis would be valuable. Recently there have been a few reports on fabricating fluorescent QDs from natural foods such as rice husk,<sup>69</sup> honey,<sup>70</sup> glucose,<sup>71</sup> milk,<sup>72</sup> orange juice<sup>73</sup> and coffee<sup>74</sup> due to their low cost, easy availability, and nearly unlimited sources.

These results inspired us to further produce fluorescent GQDs from natural foods. In this work, a selective fluorescence sensor for speciation of iron was developed based on graphene quantum dots, functionalized with glutathione (GSH-GQDs) prepared from lime oil extract. The lime oil extract was pyrolyzed in the presence of glutathione (GSH) to prepare N and S co-doped graphene quantum dots (GSH-GQDs). In the presence of ferric ion ( $\text{Fe}^{3+}$ ), the fluorescence intensity of the GSH-GQDs decreased linearly with increasing  $\text{Fe}^{3+}$  concentration due to quenching. The detection of  $\text{Fe}^{2+}$  is similar to the procedure mentioned for the determination of  $\text{Fe}^{3+}$  with the difference being the addition of  $\text{H}_2\text{O}_2$  to the sample as an oxidation agent. This is intended to be used as a fluorescence sensor for the determination of  $\text{Fe}^{2+}$  and  $\text{Fe}^{3+}$  ions. In addition, the optimum conditions including  $\text{Fe}^{2+}$ ,  $\text{Fe}^{3+}$  and  $\text{H}_2\text{O}_2$  concentration and the pH of the solution were investigated.

## 2. Experimental

### 2.1 Chemicals

All chemicals are of analytical grade. Citric acid, sodium acetate, sodium chloride, iron(II) sulfide, iron(III) chloride hexahydrate and paraffin oil were purchased from QRec™ (New Zealand). Sodium hydroxide, silver chloride, magnesium chloride, manganese(II) sulfate monohydrate, nickel(II) chloride and aluminium chloride were purchased from Carlo Erba (Italy). L-Glutathione (reduced form), mercury nitrate, cobalt nitrate hexahydrate, lead nitrate, zinc nitrate hexahydrate, cadmium nitrate tetrahydrate, copper nitrate trihydrate, and ethylenediaminetetraacetic acid (EDTA) were purchased from Sigma-Aldrich (Germany). Acetic acid was purchased from Merck (Germany). Hydrogen peroxide was purchased from Ajax Finechem (Australia). A Millipore water purification system (Molsheim, France) was used to obtain deionized water with a resistivity of 18.2 M $\Omega$  cm.

### 2.2 Instruments

Spectrofluorometer Model RF-5301PC (Shimadzu, Japan) was mainly used. UV-visible spectrophotometer Model Agilent 8453 was from Agilent (Germany). pH meter UB-10 UltraBasic (Denver, USA) was used for the solution pH buffering system. Attenuated total reflectance-Fourier transform infrared (ATR-FTIR) spectroscopic measurement was performed on a TENSOR 27 system Fourier transform infrared spectrometer (Bruker, Germany). EDX spectra were taken by a HITACHI S-3000N scanning electron microscope (SEM, Hitachi Co. Ltd., Japan).

### 2.3 Preparation and characterization of graphene quantum dots (GQDs) from lime oil extract

GQDs from citrus oil extract were prepared by pyrolysis. In this typical procedure, 130 mL of lime juice was evaporated to obtain lime oil extract. Then 2.0 g of the oil extract was added into a 5 mL beaker. The beaker was heated to 260 °C using a paraffin oil bath for about 5 min. The liquid was then transferred into a beaker containing 100 mL of 0.25 mol L<sup>−1</sup> NaOH with



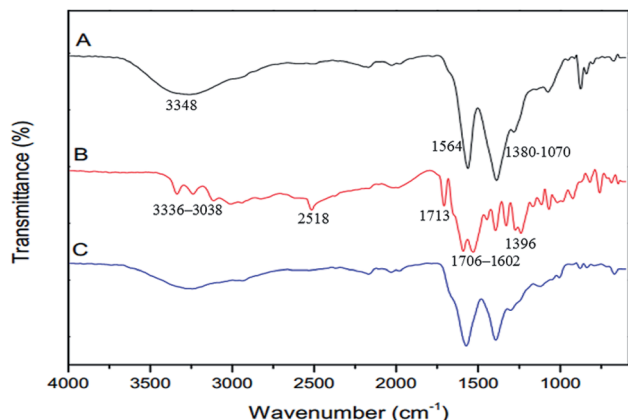


Fig. 1 FTIR spectra of (A) GQDs, (B) GSH and (C) GSH-GQDs.

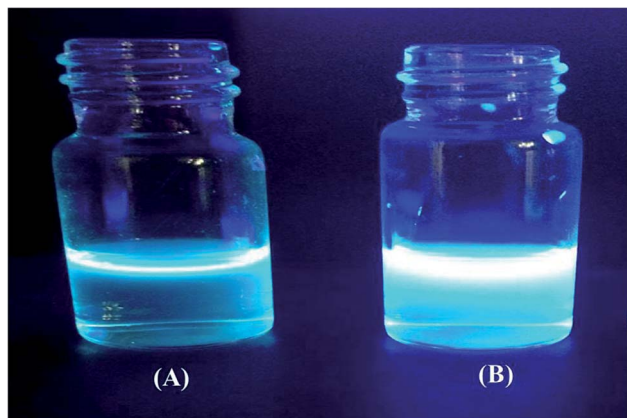


Fig. 2 The blue emission of (A) GQDs and (B) GSH-GQDs under UV light.

continuous stirring for 30 min. The obtained sample solution was neutralized to pH 7.0 with NaOH, and the GQD stock solution was stored at 4 °C before use.

## 2.4 Preparation of graphene quantum dots functionalized with glutathione (GSH-GQDs)

GSH-GQDs were also prepared by pyrolysis. Briefly, 2.0 g of lime oil extract and 1% (w/w) glutathione were added into a 5 mL beaker. The beaker was heated to 260 °C using a paraffin oil bath for about 5 min. The lime oil extract and glutathione mixture was slowly liquated and turned a brown colour. The liquid was transferred into a beaker containing 100 mL of 0.25 mol L<sup>-1</sup> NaOH with continuous stirring for 30 min. The GSH-GQD stock solution was stored at 4 °C before use.

## 2.5 Fluorescence measurement

The fluorescence measurement of GSH-GQDs was performed in acetate buffer solution at pH 4. For the determination of Fe<sup>3+</sup>, 500 µL of GSH-GQD solution and 1 mL of 1.0 M acetate buffer at pH 4 were mixed in a 10 mL volumetric flask. Then, various concentrations of Fe<sup>3+</sup> were added to an aliquot of the GSH-GQD solution (10 mL final volume) at room temperature. The Fe<sup>3+</sup> species that quenched the fluorescence intensity of each GSH-GQD solution were recorded immediately at 430 nm when excited at 345 nm. Then, the spectral measurements were used to plot the quenching calibration curve for Fe<sup>3+</sup>. The detection of Fe<sup>2+</sup> species was also done by a similar procedure to that mentioned for the determination of Fe<sup>3+</sup> with the difference being the addition of H<sub>2</sub>O<sub>2</sub> as an oxidizing agent to the sample solution.

## 2.6 Optimization of the proposed fluorescence sensor

To obtain the optimized conditions of the proposed fluorescence sensor, the main experimental parameters affecting the fluorescence intensity of the GSH-GQDs were investigated in detail as follows.

**2.6.1 Effect of pH.** The effect of the solution pH towards the fluorescence quenching of GSH-GQDs by Fe<sup>3+</sup> was studied. The experiment was carried out by adjusting 1.0 M buffer solution

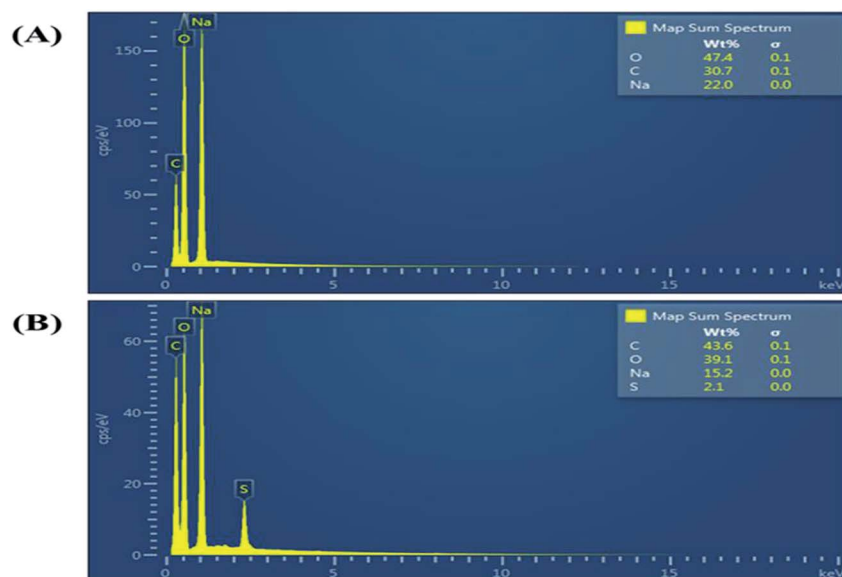


Fig. 3 EDX spectra of (A) GQDs and (B) GSH-GQDs.



(pH 2–10) containing 500  $\mu\text{L}$  of GSH-GQD solution and 25  $\mu\text{M}$  of  $\text{Fe}^{3+}$  (or  $\text{Fe}^{2+}$ ) to the desired pH solution.

**2.6.2 Effect of  $\text{H}_2\text{O}_2$  concentration.** The effect of  $\text{H}_2\text{O}_2$  concentration was tested by an evaluation of the fluorescence intensity of the GSH-GQDs. To a 10 mL volumetric flask containing 500  $\mu\text{L}$  of the GSH-GQD solution, various amounts of  $\text{H}_2\text{O}_2$  and  $\text{Fe}^{2+}$  were added and the solution was adjusted to 10 mL prior to fluorescence measurement in order to achieve solutions with final concentrations of 5, 10, 25, 50, 75 and 100  $\mu\text{M}$   $\text{H}_2\text{O}_2$  and 100  $\mu\text{M}$  of  $\text{Fe}^{2+}$ . According to the results, the concentration of  $\text{H}_2\text{O}_2$  required for the complete oxidation of  $\text{Fe}^{2+}$  did not noticeably change the fluorescence intensity of the GSH-GQDs.

**2.6.3 Effects of ionic strength and masking agent.** Various concentrations of 0.05, 0.10, 0.25, 0.20 and 0.25 M NaCl were added into 100  $\text{mg L}^{-1}$  GSH-GQD solution and adjusted to 10 mL in a volumetric flask prior to fluorescence measurement. In the same manner, 0.01, 0.02, 0.03, 0.04 and 0.05 M EDTA was added into the GSH-GQD solution and fluorescence spectra were recorded. The results were compared and discussed.

**2.6.4 Selectivity of the proposed fluorescence sensor.** To evaluate the selectivity of the proposed fluorescence sensor, the following procedure was carried out. An individual stock solution of various metal ions (10 mM) was prepared by dissolution of a metal salt in deionized water. To a 10 mL volumetric flask containing 500  $\mu\text{L}$  of the GSH-GQD solution was added 0.1 mL of 10 mM of the metal ion (final concentration of 100  $\mu\text{M}$ ) and the solution was adjusted to 10 mL with deionized water prior to fluorescence measurement.

**2.6.5 Method validation of the proposed fluorescence sensor.** The proposed fluorescence sensor was validated according to the following analytical features of merit: linearity, limit of detection (LOD), limit of quantitation (LOQ), precision (% RSD), and accuracy (% recovery).

## 3. Results and discussion

### 3.1 Characterization of the as-synthesized GQDs and GSH-GQDs

The FTIR spectra of GQDs, GSH, and GSH-GQDs are shown in Fig. 1. The as-prepared GQDs (Fig. 1A) show peaks at  $1564\text{ cm}^{-1}$ , which indicates the presence of the  $\text{C}=\text{C}$  stretching mode of polycyclic aromatic hydrocarbons.<sup>75</sup> A broad peak at  $3348\text{ cm}^{-1}$  is the characteristic peak of the hydroxyl group ( $-\text{OH}$ ) from water molecules and carboxylic groups. The  $1380\text{--}1070\text{ cm}^{-1}$  are attributed to the  $\text{C}-\text{O}$  in  $\text{COH}/\text{COC}$  (epoxy) groups.<sup>76</sup> These results

confirm the GQDs were successfully synthesized by lime oil extract pyrolysis. The FTIR spectrum of GSH is shown in Fig. 1B. Characteristic GSH broad absorption bands around  $1706\text{--}1602\text{ cm}^{-1}$  (symmetric  $\text{COO}^-$ ),  $1396\text{ cm}^{-1}$  (asymmetric  $\text{COO}^-$ ) and  $1713\text{ cm}^{-1}$  ( $\text{C}=\text{O}$ ) are observed indicating a  $-\text{COOH}$  group is present. Peaks around  $3336\text{--}3038\text{ cm}^{-1}$  indicate symmetric  $\text{N}-\text{H}$  stretching and  $2518\text{ cm}^{-1}$  indicate  $-\text{SH}$  ( $\text{S}-\text{H}$ ) groups,<sup>77</sup> respectively. In the FTIR spectra of GQDs functionalized with GSH (Fig. 1C), the disappearance of the  $\text{S}-\text{H}$  group vibration at  $2518\text{ cm}^{-1}$  ( $\text{S}-\text{H}$ ) is clear and is likely a consequence of a covalent bond established between the GQDs and GSH. These spectra confirmed the presence of GSH doped in the GQDs.

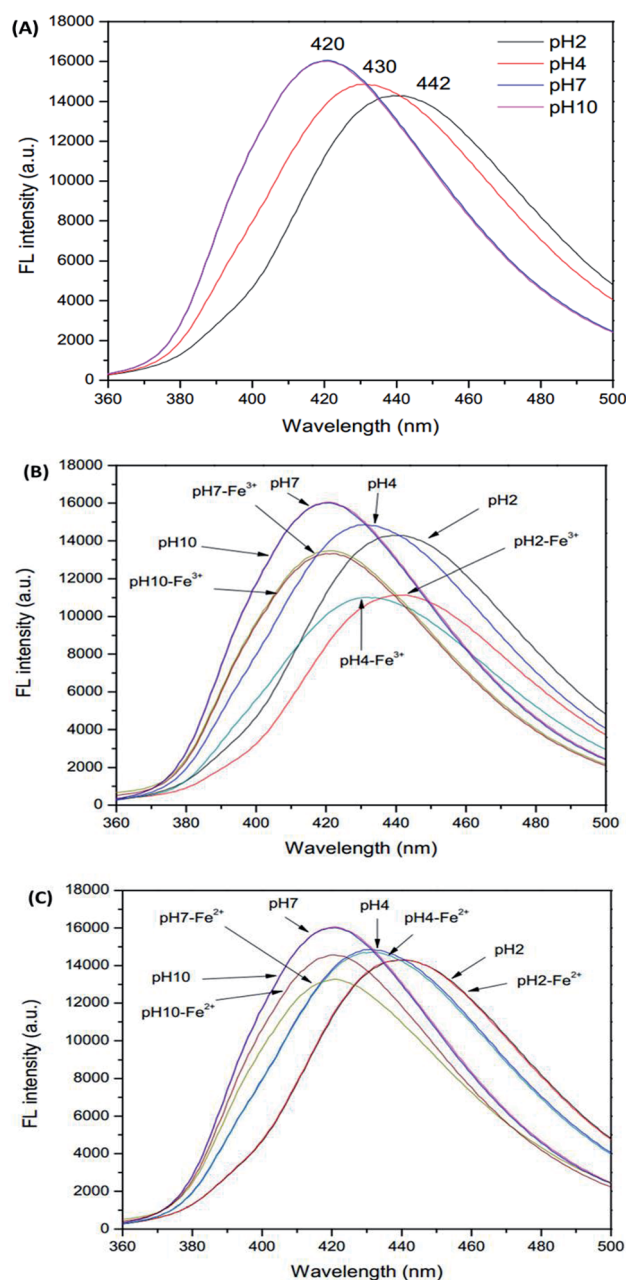
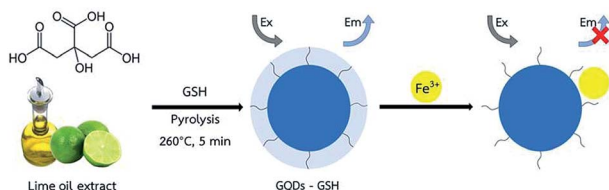


Fig. 4 Effect of pH on (A) GSH-GQDs, (B) GSH-GQDs- $\text{Fe}^{3+}$  and (C) GSH-GQDs- $\text{Fe}^{2+}$ .



Scheme 1 Schematic diagram for synthesizing GSH doped GQDs and their application in  $\text{Fe}^{3+}$  detection.





Fig. 2 shows a photograph of the solution of GQDs Fig. 2(A) and GSH-GQDs Fig. 2(B) taken under UV light. The GSH-GQD solution shows brighter blue emission than the GQDs under UV light. It was also confirmed by EDX spectra (Fig. 3A and B) that the GSH doped GQDs, compared with bare GQDs, were obtained by the appearance of S at 2.31 keV (Fig. 3B) which was commonly found in association with C (0.277 keV) and O (0.525 keV), but not N (0.392 keV) which would be a weak signal and overlapped in between the C and O peaks. The presence of the Na peak in both EDX spectra came from the NaOH solution used.

### 3.2 The fluorescence turn-off sensor for ferric ions with GSH-GQDs

The overall assay strategy for the sensing of  $\text{Fe}^{3+}$  is shown in Scheme 1. GSH doped GQDs were obtained through the pyrolysis of lime oil extract in the presence of GSH at 260 °C for 5 min, in which the GSH was used as an additional sulfur and nitrogen source, while the lime oil extract was used as the natural carbon source. The absorption and emission fluorescence spectra of GSH-GQDs show peaks at 345 and 430 nm, respectively. The GSH-GQDs show excellent fluorescence stability and low toxicity under the preparation conditions.

More importantly, it was demonstrated that the GSH-GQDs were highly selective towards  $\text{Fe}^{3+}$ , in which it is evident that the incorporation of S atoms into GQDs should be of crucial importance for tuning the electronic local density of the GQDs and promoting the coordination interaction between  $\text{Fe}^{3+}$  and the phenolic hydroxyl groups on the edge of S-GQDs. S

(electronegativity of S: 2.58) is an electron donor, but fundamentally different from N (electronegativity of N: 3.04) because of its lower electronegativity and larger atomic radius. Therefore, the valence electrons of S in the third shell are easily lost, and the higher surface electron density of O atoms further promotes the coordination interaction.<sup>78</sup> Therefore, we deduce that when  $\text{Fe}^{3+}$  ions are added into the S-GQDs solution, they can coordinate with the phenolic hydroxyl groups on the edge of S-GQDs, and the electrons in the excited state of S-GQDs will transfer to the half-filled 3d orbitals of  $\text{Fe}^{3+}$ , facilitating non-radiative electron/hole recombination annihilation and leading to significant fluorescence quenching.<sup>79,80</sup>

### 3.3 Effect of the solution pH

Initially, due to the presence of pH sensitive functional groups in the GSH-GQDs, we investigated the effect of pH on their fluorescence intensity. As demonstrated in Fig. 4A–C, we found that the pH of the solution is able to influence the fluorescence signal of the sensor before and after the addition of  $\text{Fe}^{3+}$  ions. The fluorescence intensity of the sensor is plotted *versus* pH in the range of 2–10 (Fig. 4A). It was observed that the emission intensity changed the maximum wavelength and decreased sharply when the pH value was below 7. It was evident that at various pH values the fluorescence intensity was quenched by  $\text{Fe}^{3+}$ , but at around pH 4 it could not be quenched by  $\text{Fe}^{2+}$ . Thus, towards this sensitive pH value an iron speciation analysis could be selectively conducted in association with simple oxidation of  $\text{Fe}^{2+}$  to  $\text{Fe}^{3+}$  using  $\text{H}_2\text{O}_2$  as an oxidizing agent.

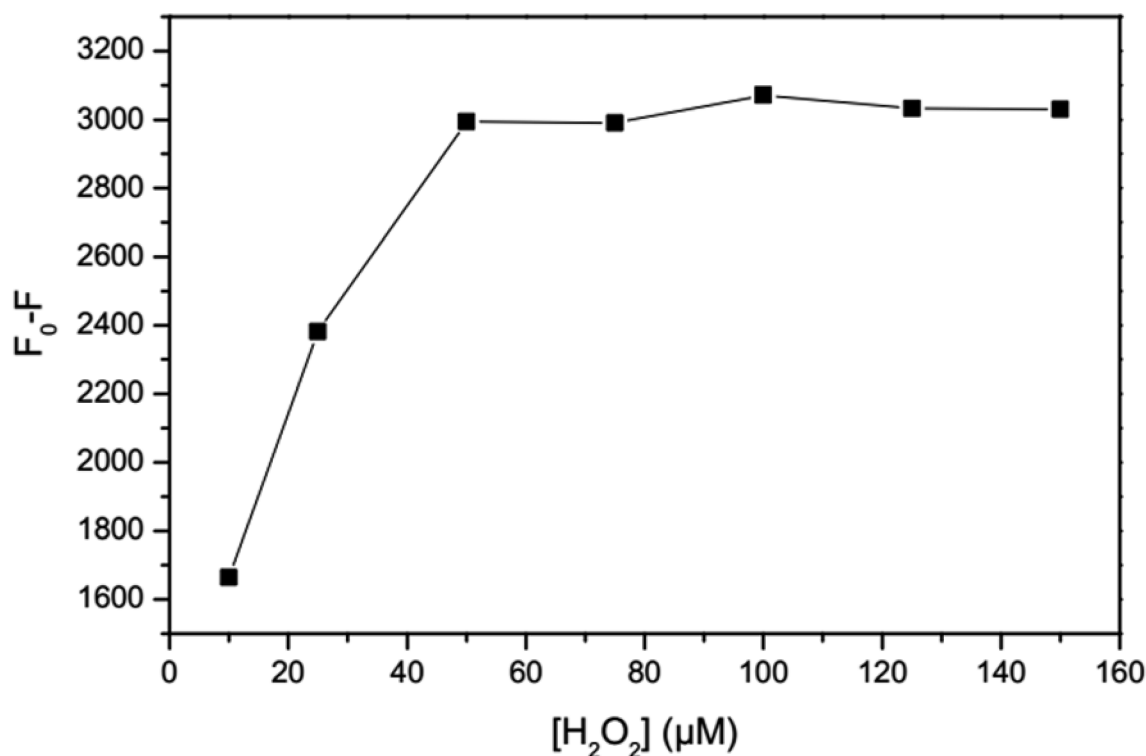


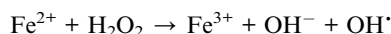
Fig. 5 Effect of  $\text{H}_2\text{O}_2$  concentration.



In order to keep the fluorescence intensity of the GSH-GQDs as stable as possible and to ensure sensitive determination of  $\text{Fe}^{3+}$ , a citrate buffer solution (pH 4, 1.0 M) was used.

### 3.4 Effect of $\text{H}_2\text{O}_2$ on speciation of $\text{Fe}^{2+}$ and $\text{Fe}^{3+}$

Our studies showed that  $\text{Fe}^{3+}$  ions immediately reduce the fluorescence intensity of GSH-GQDs. However, no such changes were observed when  $\text{Fe}^{3+}$  was replaced by  $\text{Fe}^{2+}$ . According to the following reaction,  $\text{H}_2\text{O}_2$  is capable of generating higher oxidation states of iron, which is referred to as the Fenton reaction.<sup>81</sup>



Therefore, by means of the Fenton reaction, selective and sensitive determination of  $\text{Fe}^{2+}$  based on GSH-GQDs fluorescence quenching is feasible. The effect of  $\text{H}_2\text{O}_2$  concentration was tested by evaluating the fluorescence intensity of the GSH-GQDs.

As shown in Fig. 5, the addition of  $\text{H}_2\text{O}_2$  results in quenching of the fluorescence intensity proportional to the  $\text{H}_2\text{O}_2$

concentration. The optimum concentration of hydrogen peroxide is when no obvious change in fluorescence intensity due to  $\text{H}_2\text{O}_2$  is observed in the absence of  $\text{Fe}^{2+}$ , while in the presence of  $\text{Fe}^{2+}$  oxidation of almost all of the  $\text{Fe}^{2+}$  ions occurs. Therefore, the effectiveness of different concentrations of  $\text{H}_2\text{O}_2$  for oxidation of the highest concentration of  $\text{Fe}^{2+}$  in a linear range (100  $\mu\text{M}$ ) was investigated. According to the revealed

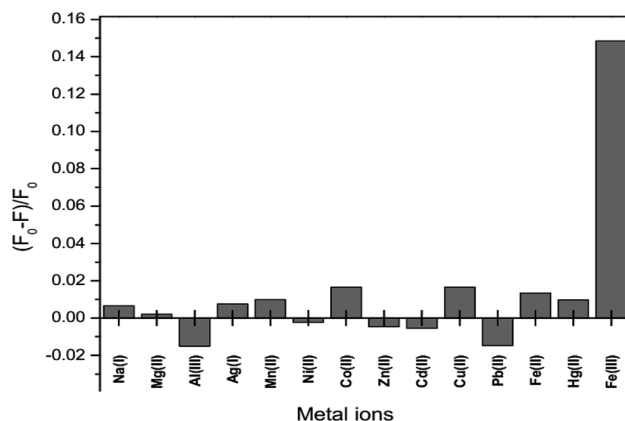


Fig. 8 Fluorescence response of GSH-GQDs to various metal cations with a concentration of 10  $\mu\text{M}$ .

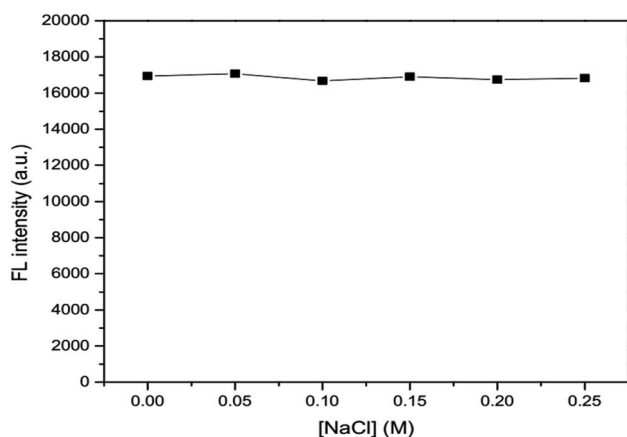


Fig. 6 Effect of concentration of NaCl as an ionic strength.

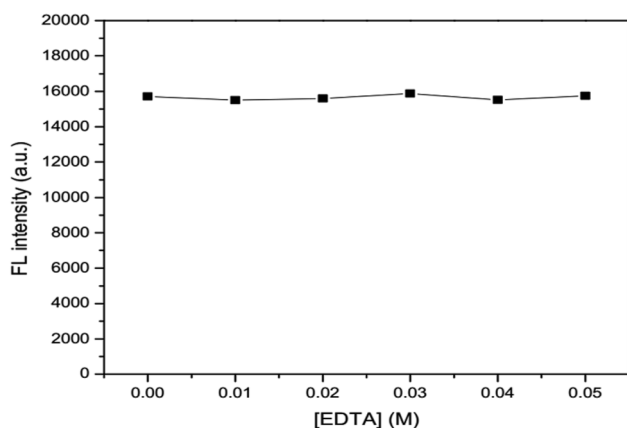


Fig. 7 Effect of concentration of EDTA as a masking agent.

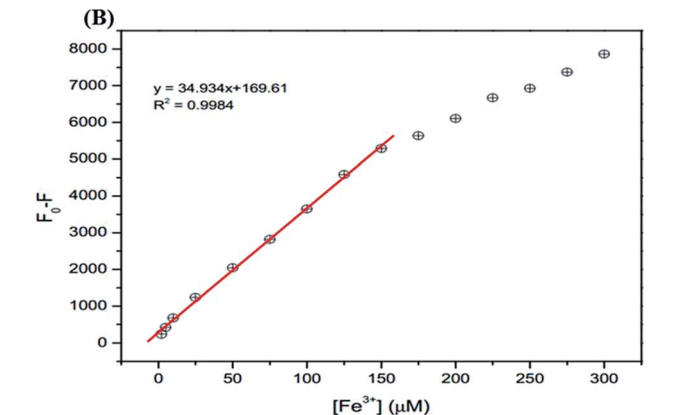
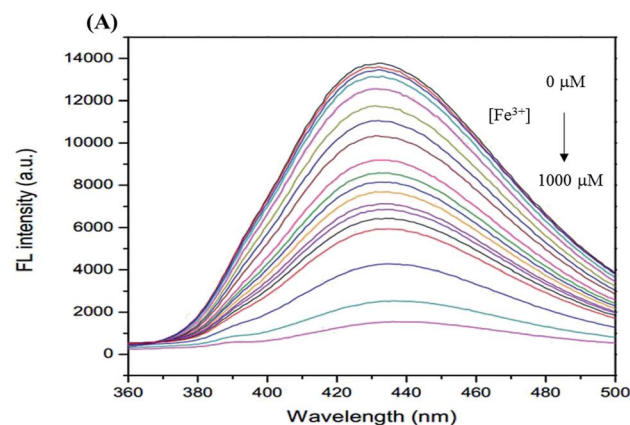


Fig. 9 (A) The changes in the FL intensity of the GSH-GQDs at different  $\text{Fe}^{3+}$  concentrations (0–1000  $\mu\text{M}$ ), (B) linear relationship of  $F_0 - F$  versus the concentration of  $\text{Fe}^{3+}$  over the range 1–150  $\mu\text{M}$ .



results, the concentration of 50  $\mu\text{M}$  was chosen for  $\text{H}_2\text{O}_2$ , taking the complete oxidation of  $\text{Fe}^{2+}$  ions and unnoticeable change of GSH-GQDs emission into account.

### 3.5 Effect of ionic strength and masking agent

The effects of ionic strength as 0.05, 0.10, 0.15, 0.20 and 0.25 M NaCl solutions (Fig. 6) and masking agent as 0.01, 0.02, 0.03, 0.04 and 0.05 EDTA solutions (Fig. 7) tested were also investigated. It was found that both ionic strength and masking agent had no effect on the fluorescence intensity of the GSH-GQD solution. A further aim is that modification of the ionic strength of the mixture solution could be done in association with the addition of EDTA to mask any metal ion interferences in the sample.

### 3.6 Selectivity of the proposed sensor

The fluorescence intensity of GSH-GQDs in the presence of various metal ions,  $\text{Na}^+$ ,  $\text{Ag}^+$ ,  $\text{Mg}^{2+}$ ,  $\text{Mn}^{2+}$ ,  $\text{Ni}^{2+}$ ,  $\text{Co}^{2+}$ ,  $\text{Zn}^{2+}$ ,  $\text{Cd}^{2+}$ ,  $\text{Cu}^{2+}$ ,  $\text{Pb}^{2+}$ ,  $\text{Fe}^{2+}$ ,  $\text{Hg}^{2+}$ ,  $\text{Al}^{3+}$  and  $\text{Fe}^{3+}$ , was investigated. The values of  $(F_0 - F)/F_0$  were plotted using 0.1 mL of 10  $\mu\text{M}$  of each metal. Fig. 8 shows that the addition of  $\text{Fe}^{3+}$  to the reaction mixture of the GSH-GQDs system resulted in fluorescence quenching, whereas the other remaining cations had no significant effect under the same experimental conditions.

### 3.7 Method validation

The analytical characteristics of the proposed method were validated under optimized conditions in terms of linearity, limit

of detection (LOD), limit of quantification (LOQ), and precision (expressed as the relative standard deviation, RSD, of the calibration slope obtained from both intra-day and inter-day analysis) to estimate the efficiency and feasibility of the method for use with drinking water samples. The linearity range is from 1–150  $\mu\text{M}$  ( $R^2 = 0.9984$ ). The linear calibration graph is as follows:  $y = 34.934x + 169.61$  (where  $y$  is the fluorescence intensity and  $x$  is the concentration of  $\text{Fe}^{3+}$ ) (Fig. 9). The LOD defined as  $3\text{SD}/m$  (where SD is the standard deviation of a very low concentration of  $\text{Fe}^{3+}$  and  $m$  is the slope of the calibration graph) was 0.10  $\mu\text{M}$ . The LOQ defined as  $10\text{SD}/m$ , was 0.34  $\mu\text{M}$ . The precision, which was evaluated in terms of repeatability (data from  $3 \times 3$  independent standard preparation, intra-day RSD), was 2.03% and 3.17% and the reproducibility (work performed during  $5 \times 3$  consecutive days, inter-day RSD) was 3.11% and 4.55% for  $\text{Fe}^{2+}$  and  $\text{Fe}^{3+}$ , respectively, indicating acceptable repeatability of the method.

### 3.8 Real sample analysis

Iron speciation,  $\text{Fe}^{2+}$  and  $\text{Fe}^{3+}$ , in some brands of bottled drinking water samples was studied. To demonstrate the applicability and reliability of the proposed method, it was successfully applied to fifteen samples of drinking water including five brands of water (brands 1–5). The amounts of  $\text{Fe}^{2+}$  and  $\text{Fe}^{3+}$  in these samples were obtained as shown in Table 1. The results showed that both  $\text{Fe}^{2+}$  and  $\text{Fe}^{3+}$  were found in all samples studied. In addition, to evaluate the matrix effect the accuracy of the method was verified by calculating the recovery in the real samples. Each sample was spiked with five

Table 1 The amount and recovery of  $\text{Fe}^{2+}$  and  $\text{Fe}^{3+}$  in drinking water samples using the GQDs-GSH system ( $n = 3$ )

Drinking water sample	$\text{Fe}^{2+}$			$\text{Fe}^{3+}$		
	Added ( $\mu\text{M}$ )	Found ( $\mu\text{M}$ )	Recovery (%) $\pm$ SD	Added ( $\mu\text{M}$ )	Found ( $\mu\text{M}$ )	Recovery (%) $\pm$ SD
Brand 1	0	0.11	—	0	0.22	—
	25	25.72	$102.86 \pm 4.15$	25	25.22	$100.90 \pm 1.85$
	50	51.15	$102.30 \pm 1.08$	50	49.04	$98.08 \pm 2.67$
	75	75.95	$101.27 \pm 3.13$	75	75.17	$100.23 \pm 2.54$
	100	103.24	$103.24 \pm 4.44$	100	98.55	$98.55 \pm 4.34$
Brand 2	0	0.28	—	0	0.34	—
	25	25.51	$102.05 \pm 3.73$	25	25.28	$101.13 \pm 1.89$
	50	51.04	$102.07 \pm 2.58$	50	49.99	$99.99 \pm 3.73$
	75	78.06	$104.09 \pm 2.24$	75	74.45	$99.26 \pm 5.20$
	100	103.01	$103.01 \pm 4.11$	100	98.20	$98.20 \pm 2.97$
Brand 3	0	0.40	—	0	0.37	—
	25	25.17	$100.66 \pm 2.99$	25	25.05	$100.20 \pm 2.69$
	50	51.88	$103.75 \pm 4.34$	50	49.39	$98.77 \pm 2.49$
	75	77.69	$103.58 \pm 2.61$	75	74.77	$99.69 \pm 3.15$
	100	101.13	$101.13 \pm 3.92$	100	100.06	$100.06 \pm 2.56$
Brand 4	0	0.25	—	0	0.42	—
	25	25.02	$100.09 \pm 3.44$	25	25.57	$102.29 \pm 4.22$
	50	50.78	$101.55 \pm 4.22$	50	51.33	$102.65 \pm 2.09$
	75	76.62	$102.16 \pm 3.17$	75	74.30	$99.07 \pm 5.11$
	100	102.55	$102.55 \pm 1.97$	100	99.13	$99.13 \pm 3.42$
Brand 5	0	0.16	—	0	0.31	—
	25	25.08	$100.32 \pm 3.59$	25	25.31	$101.24 \pm 3.12$
	50	51.24	$102.48 \pm 2.99$	50	50.83	$101.67 \pm 2.41$
	75	77.28	$103.04 \pm 3.18$	75	75.69	$100.92 \pm 2.38$
	100	102.31	$102.31 \pm 3.75$	100	99.51	$99.51 \pm 1.86$



**Table 2** Selected chemical sensors using carbon based materials for the determination of Fe<sup>2+</sup> and Fe<sup>3+</sup> ions

Carbon based material	Linear range	LOD	Reference
Carbon dots (CDs) conjugated with phenol groups	1–100 mM	0.17 mM	82
Gold nanoparticles (AuNPs) conjugated with glycol chitosan	0–180 μM	11.3 nM	83
Boron-doped graphene quantum dots (B-GQDs)	0.01–100 μM	0.005 μM	84
Sulfur-doped graphene quantum dots (S-GQDs)	0–0.70 μM	4.2 nM	85
Nitrogen-doped carbon dots (N-CDs)	0–1.6 μM	0.05 μM	86
N/P co-doped carbon dots	1–150 μM	0.33 μM	87
GSH-doped GQDs (lime oil extract)	1–150 μM	0.10 μM	This work

concentrations (0, 25, 50, 75 and 100 μM) of a standard solution of both Fe<sup>2+</sup> and Fe<sup>3+</sup>. Then, the relative percentage recoveries were calculated as follows:

$$\% \text{ Recovery} = [(C_{\text{found}} - C_{\text{real}})/C_{\text{added}}] \times 100$$

where,  $C_{\text{found}}$ ,  $C_{\text{real}}$  and  $C_{\text{added}}$  are the concentration of analyte after addition of a known amount of standard to the real sample, the concentration of analyte in the real sample, and the concentration of the known amount of standard that was spiked in real sample, respectively. From the results (Table 1), it was found that the recoveries of the proposed method expressed as the mean percentage ( $n = 3$ ) were in the range of 100.09–104.09% and 98.08–102.65% for Fe<sup>2+</sup> and Fe<sup>3+</sup>, respectively. This demonstrates that this method provides acceptable recovery for the determination of both Fe<sup>2+</sup> and Fe<sup>3+</sup> in real samples. Therefore, it is concluded that the matrix effect on the performance of the proposed method in these samples is negligible. The sensing property, particularly expressed as LOD, of the developed method is compared with those of selected relevant reports as shown in Table 2.<sup>82–87</sup>

## 4. Conclusion

A highly sensitive fluorescence sensor for speciation of Fe<sup>2+</sup> and Fe<sup>3+</sup> ions based on the fluorescence quenching of GSH-GQDs was obtained. A novel approach for the preparation of GQDs by pyrolysis of citric acid rich-lime oil extract was demonstrated for selective determination of Fe<sup>2+</sup> and Fe<sup>3+</sup> at trace level under optimum conditions, mainly including ensuring the solution was pH 4.0 in the presence of H<sub>2</sub>O<sub>2</sub>. The analytical features of merit of the proposed method were well validated, and could be applied to determine both Fe<sup>2+</sup> and Fe<sup>3+</sup> in five brands of bottled drinking water samples, in particular having high recovery. Using the as-prepared GQDs doped with a small amount of GSH as a simple and cheap fluorescence sensor with natural lime oil extract as a starting material meets the requirements of green chemistry. In addition, using multi-functional materials such as a S- and N-doped GQD based spectroscopic sensor and/or other reactive cation or anion-doped carbon based materials with their intrinsic quantum yields could have potential in approaching green chemistry for future trends in nanoparticle applications.<sup>88–90</sup>

## Conflicts of interest

The authors have declared no conflict of interest.

## Acknowledgements

The authors thank the Higher Education Research Promotion and National Research University Project of Thailand, Office of the Higher Education Commission, through the Food and Functional Food Research Cluster of Khon Kaen University, Materials Chemistry Research Center, Department of Chemistry and Center of Excellence for Innovation in Chemistry (PERCH-CIC), Thailand for financial support.

## References

- 1 M. W. Hentze, M. U. Muckenthaler, B. Galy and C. Camaschella, *Cell*, 2010, **142**, 24–38.
- 2 T. A. Rouault, *Nat. Chem. Biol.*, 2006, **2**, 406–414.
- 3 B. D'Autreaux, N. P. Tucker, R. Dixon and S. Spiro, *Nature*, 2005, **437**, 769–772.
- 4 J. S. Wu, W. M. Liu, J. C. Ge, H. Y. Zhang and P. F. Wang, *Chem. Soc. Rev.*, 2011, **40**, 3483–3495.
- 5 R. S. Eisenstein, *Annu. Rev. Nutr.*, 2000, **20**, 627–662.
- 6 M. Balcerzak and A. Tyburska, *Acta Pharm.*, 2008, **58**, 327–334.
- 7 S. X. Wang, X. M. Meng and M. Z. Zhu, *Tetrahedron Lett.*, 2011, **52**, 2840–2843.
- 8 C. Brugnara, *Clin. Chem.*, 2003, **49**, 1573–1578.
- 9 N. Narayanaswamy and T. Govindaraju, *Sens. Actuators, B*, 2012, **161**, 304–310.
- 10 World Health Organization, Water safety plans, in *WHO Guidelines for Drinking Water Quality*, WHO, Geneva, 4th edn, 2011, p. 226, [http://whqlibdoc.who.int/publications/2011/9789241548151\\_eng.pdf](http://whqlibdoc.who.int/publications/2011/9789241548151_eng.pdf).
- 11 Y. Chen, Y. Huang, S. Feng and D. Yuan, *Anal. Methods*, 2015, **7**, 4971–4978.
- 12 Y. H. He, J. P. Lai, H. Sun, Z. M. Chen and S. Lan, *Sens. Actuators, B*, 2016, **225**, 405–412.
- 13 L. K. Mudashiru, A. C. Aplin and B. R. Horrocks, *Anal. Methods*, 2011, **3**, 927–936.
- 14 P. Bermejo, E. Peña, R. Domínguez, A. Bermejo, J. M. Fraga and J. A. Cocho, *Talanta*, 2000, **50**, 1211–1222.
- 15 J. Xu, P. Che and Y. F. Ma, *J. Chromatogr. A*, 1996, **749**, 287–294.
- 16 X. P. Yan, M. J. Hendry and R. Kerrich, *Anal. Chem.*, 2000, **72**, 1879–1884.
- 17 A. Saavedra, E. Donati and E. Cortón, *Sens. Actuators, B*, 2015, **220**, 448–455.





- 18 S. Hirata, H. Yoshihara and M. Aihara, *Talanta*, 1999, **49**, 1059–1067.
- 19 M. Karimil, A. Badieil and G. M. Ziarani, *J. Fluoresc.*, 2015, **25**, 1297–1302.
- 20 R. Kagit, M. Yildirim, O. Ozay, S. Yesilot and H. Ozay, *Inorg. Chem.*, 2014, **53**, 2144–2151.
- 21 B.-Y. Chen, C.-C. Kuo, Y.-S. Huang, S.-T. Lu, F.-C. Liang and D.-H. Jiang, *ACS Appl. Mater. Interfaces*, 2015, **7**, 2797–2808.
- 22 L. Tang, R. Ji, X. Cao, J. Lin, H. Jiang, X. Li, K. S. Teng, C. M. Luk, S. Zeng, J. Hao and S. P. Lau, *ACS Nano*, 2012, **6**, 5102–5110.
- 23 S. Zhuo, M. Shao and S.-T. Lee, *ACS Nano*, 2012, **6**, 1059–1064.
- 24 S. Zhu, J. Zhang, S. Tang, C. Qiao, L. Wang, H. Wang, X. Liu, B. Li, Y. Li, W. Yu, X. Wang, H. Sun and B. Yang, *Adv. Funct. Mater.*, 2012, **22**, 4732–4740.
- 25 J. Shen, Y. Zhu, C. Chen, X. Yang and C. Li, *Chem. Commun.*, 2011, **47**, 2580–2582.
- 26 D. Pan, J. Zhang, Z. Li and M. Wu, *Adv. Mater.*, 2010, **22**, 734–738.
- 27 M. Zhang, L. Bai, W. Shang, W. Xie, H. Ma, Y. Fu, D. Fang, H. Sun, L. Fan, M. Han, C. Liu and S. J. Yang, *Mater. Chem.*, 2012, **22**, 7461–7467.
- 28 Y. Wu, M. Wen, M. Navlani-García, Y. Kuwahara, K. Mori and H. Yamashita, *Chem.-Asian J.*, 2017, **12**, 860–867.
- 29 S. H. Choi, D. H. Kim, A. V. Raghu, K. R. Reddy, H.-I. Lee, K. S. Yoon, H. M. Jeong and B. K. Kim, *J. Macromol. Sci., Part B: Phys.*, 2012, **51**, 197–207.
- 30 M. U. Khan, K. R. Reddy, T. Snguanwongchai, E. Haque and V. G. Gomes, *Colloid Polym. Sci.*, 2016, **294**, 1599–1610.
- 31 B. D. Pan, J. Zhang, Z. Li and M. Wu, *Adv. Mater.*, 2010, **22**, 734–738.
- 32 K. R. Reddy, K.-P. Lee, A. I. Gopalan, M. S. Kim, A. M. Showkat and Y. C. Nho, *J. Polym. Sci., Part A: Polym. Chem.*, 2006, **44**, 3355–3364.
- 33 K. R. Reddy, V. G. Gomes and M. Hassan, *Mater. Res. Express*, 2014, **1**, 015012.
- 34 K. R. Reddy, B. C. Sin, C. H. Yoo, W. Park, K. S. Ryu, J.-S. Lee, D. Sohn and Y. Lee, *Scr. Mater.*, 2008, **58**, 1010–1013.
- 35 K. R. Reddy, B. C. Sin, K. S. Ryu, J. Noh and Y. Lee, *Synth. Met.*, 2009, **159**, 1934–1939.
- 36 H. Cheng, Y. Zhao, Y. Fan, X. Xie, L. Qu and G. Shi, *ACS Nano*, 2012, **6**, 2237–2244.
- 37 J. Shen, Y. Zhu, X. Yang and C. Li, *Chem. Commun.*, 2012, **48**, 3686–3699.
- 38 H. Tetsuka, R. Asahi, A. Nagoya, K. Okamoto, I. Tajima, R. Ohta and A. Okamoto, *Adv. Mater.*, 2012, **24**, 5333–5338.
- 39 D. R. Son, A. V. Raghu, K. R. Reddy and H. M. Jeong, *J. Macromol. Sci., Part B: Phys.*, 2016, **55**, 1099–1110.
- 40 P. Luo, Z. Ji, C. Li and G. Shi, *Chem. Commun.*, 2013, **46**, 5094–5096.
- 41 J. Shen, Y. Zhu, C. Chen, X. Yang and C. Li, *Chem. Commun.*, 2011, **47**, 2580–2582.
- 42 J. Shen, Y. Zhu, X. Yang, J. Zong, J. Zhang and C. Li, *New J. Chem.*, 2012, **36**, 97–101.
- 43 Y.-L. Zhang, L. Wang, H.-C. Zhang, Y. Liu, H.-Y. Wang, Z.-H. Kang and S.-T. Lee, *RSC Adv.*, 2013, **3**, 3733–3738.
- 44 K. R. Reddy, M. Hassan and V. G. Gomes, *Appl. Catal., A*, 2015, **489**, 1–16.
- 45 Y. R. Lee, S. C. Kim, H.-i. Lee, H. M. Jeong, A. V. Raghu, K. R. Reddy and B. K. Kim, *Macromol. Res.*, 2011, **19**, 66–71.
- 46 M. Cakici, R. R. Kakarla and F. Alonso-Marroquin, *Chem. Eng. J.*, 2017, **309**, 151–158.
- 47 F. Wang, Z. Gu, W. Lei, W. Wang, X. Xia and Q. Hao, *Sens. Actuators, B*, 2014, **190**, 516–522.
- 48 Y.-X. Qi, M. Zhang, Q.-Q. Fu, R. Liu and G.-Y. Shi, *Chem. Commun.*, 2013, **49**, 10599–10601.
- 49 L. Fan, Y. Hu, X. Wang, L. Zhang, F. Li, D. Han, Z. Li, Q. Zhang, Z. Wang and L. Niu, *Talanta*, 2012, **101**, 192–197.
- 50 Y. Zhou, Z.-B. Qu, Y. Zeng, T. Zhou and G. Shi, *Biosens. Bioelectron.*, 2014, **52**, 317–323.
- 51 F. Yang, M. Zhao, B. Zheng, D. Xiao, L. Wu and Y. Guo, *J. Mater. Chem.*, 2012, **22**, 25471–25479.
- 52 H. Zhao, Y. Chang, M. Liu, S. Gao, H. Yu and X. Quan, *Chem. Commun.*, 2013, **49**, 234–236.
- 53 Y. Wang, L. Zhang, R.-P. Liang, J.-M. Bai and J.-D. Qiu, *Anal. Chem.*, 2013, **85**, 9148–9155.
- 54 D. Pan, J. Zhang, Z. Li and M. Wu, *Adv. Mater.*, 2010, **22**, 734–738.
- 55 S. Zhu, J. Zhang, C. Qiao, S. Tang, Y. Li, W. Yuan, B. Li, L. Tian, F. Liu, R. Hu, H. Gao, H. Wei, H. Zhang, H. Sun and B. Yang, *Chem. Commun.*, 2011, **47**, 6858–6860.
- 56 L. Lin and S. Zhang, *Chem. Commun.*, 2012, **48**, 10177–10179.
- 57 Y. Li, Y. Zhao, H. Cheng, Y. Hu, G. Shi, L. Dai and L. Qu, *J. Am. Chem. Soc.*, 2012, **134**, 15–18.
- 58 C. Hu, Y. Liu, Y. Yang, J. Cui, Z. Huang, Y. Wang, L. Yang, H. Wang, Y. Xiao and J. Rong, *J. Mater. Chem. B*, 2013, **1**, 39–42.
- 59 Q. Liu, B. Guo, Z. Rao, B. Zhang and J. R. Gong, *Nano Lett.*, 2013, **13**, 2436–2441.
- 60 Z. Fan, Y. Li, X. Li, L. Fan, S. Zhou, D. Fang and S. Yang, *Carbon*, 2014, **70**, 149–156.
- 61 D. Qu, M. Zheng, P. Du, Y. Zhou, L. Zhang, D. Li, H. Tan, Z. Zhao, Z. Xie and Z. Sun, *Nanoscale*, 2013, **5**, 12272–12277.
- 62 S. Li, Y. Li, J. Cao, J. Zhu, L. Fan and X. Li, *Anal. Chem.*, 2014, **86**, 10201–10207.
- 63 D. Pan, J. Zhang, Z. Li and M. Wu, *Adv. Mater.*, 2010, **22**, 734–737.
- 64 R. Liu, D. Wu, X. Feng and K. Muellen, *J. Am. Chem. Soc.*, 2011, **133**, 15221–15223.
- 65 J. Peng, W. Gao, B. K. Gupta, Z. Liu, R. A. RomeroBurto, L. Ge, L. Song, L. B. Alemany, X. Zhan, G. Gao, S. A. Vithayathil, B. A. Kaiparettu, A. A. Marti, T. Hayashi, J. J. Zhu and P. M. Ajayan, *Nano Lett.*, 2012, **12**, 844–849.
- 66 Y. Dong, J. Lin, Y. Chen, F. Fu, Y. Chi and G. Chen, *Nanoscale*, 2014, **6**, 7410–7415.
- 67 Y. Dong, J. Shao, C. Chen, H. Li, R. Wang, Y. Chi, X. Lin and G. Chen, *Carbon*, 2012, **50**, 4738–4743.
- 68 Z. Wang, J. Yu, X. Zhang, N. Li, B. Liu, Y. Li, Y. Wang, W. Wang, Y. Li, L. Zhang, S. Dissanayake, S. L. Suib and L. Sun, *ACS Appl. Mater. Interfaces*, 2016, **8**, 1434–1439.
- 69 S. Mahesh, C. L. Lekshmi, K. D. Renuka and K. Joseph, *Part. Part. Syst. Charact.*, 2016, **30**, 70–74.



- 70 L. B. Tang, R. B. Ji, X. M. Li, G. X. Bai, C. P. Liu, J. H. Hao, J. Y. Lin, H. X. Jiang, K. S. Teng, Z. B. Yang and S. P. Lau, *ACS Nano*, 2014, **8**, 6312–6320.
- 71 C. Z. Zhu, J. F. Zhai and S. J. Dong, *Chem. Commun.*, 2012, **48**, 9367–9369.
- 72 S. Sahu, B. Behera, T. K. Maiti and S. Mohapatra, *Chem. Commun.*, 2012, **48**, 8835–8837.
- 73 L. Wang, W. Li, B. Wu, Z. Li, S. Wang, Y. Liu, D. Pan and M. Wu, *Chem. Eng. J.*, 2016, **300**, 75–82.
- 74 W. Zhang, Y. Liu, X. Meng, T. Ding, Y. Xu, H. Xu, Y. Ren, B. Liu, J. Huang, J. Yang and X. Fang, *Phys. Chem. Chem. Phys.*, 2015, **17**, 22361–22366.
- 75 H. Wang, Q. Hao, X. Yang, L. Lu and X. Wang, *Electrochem. Commun.*, 2009, **11**, 1158–1161.
- 76 J. P. Monrás, V. Díaz, D. Bravo, R. A. Montes, T. G. Chasteen, I. O. Osorio-Román, C. C. Vásquez and J. M. Pérez-Donoso, *PLoS One*, 2012, **7**, 48657.
- 77 S. Li, Y. Li, J. Cao, J. Zhu, L. Fan and X. Li, *Anal. Chem.*, 2014, **86**, 10201–10207.
- 78 Q. Mei, C. Jiang, G. Guan, K. Zhang, B. Liu and R. Liu, *Chem. Commun.*, 2012, **48**, 7468–7470.
- 79 Y.-S. Xia and C.-Q. Zhu, *Talanta*, 2008, **75**, 215–221.
- 80 R. Liu, H. Li, W. Kong, J. Liu, Y. Liu and C. Tong, *Mater. Res. Bull.*, 2013, **48**, 2529–2534.
- 81 H. J. H. Fenton and J. H. Ryffel, *J. Chem. Soc., Trans.*, 1902, **81**, 434.
- 82 M. R. Hormozi-Nezhad and M. Taghipoura, *Anal. Methods*, 2016, **8**, 4064–4068.
- 83 K. Kim, Y.-S. Nam, Y. Lee and K.-B. Lee, *J. Anal. Methods Chem.*, 2017, **2017**, 1–11.
- 84 L. Chen, C. Wu, P. D. Xiaowei, F. P. Wu and C. Cai, *Talanta*, 2017, **164**, 100–109.
- 85 S. Li, Y. Li, J. Cao, J. Zhu, L. Fan and X. Li, *Anal. Chem.*, 2014, **86**(20), 10201–10207.
- 86 R. Wang, X. Wang and Y. Sun, *Sens. Actuators, B*, 2017, **241**, 73–79.
- 87 J. Shangguan, J. Huang, D. He, X. He, K. Wang, R. Ye, X. Yang, T. Qing and J. Tang, *Anal. Chem.*, 2017, **89**, 7477–7484.
- 88 M. Hassan, E. Haque, K. R. Reddy, A. I. Minett, J. Chen and V. G. Gomes, *Nanoscale*, 2014, **6**, 11988–11994.
- 89 K. R. Reddy, H. M. Jeong, Y. Lee and A. V. Raghu, *J. Polym. Sci., Part A: Polym. Chem.*, 2010, **48**, 1477–1484.
- 90 K. R. Reddy, K.-P. Lee, J. Y. Kim and Y. Lee, *J. Nanosci. Nanotechnol.*, 2008, **8**, 5632–5639.

